Role of surface adsorption and porosity features in the molecular recognition ability of imprinted sol-gels

Laura Guardia[1], *Rosana Badía-Laíño*[1], *Marta-Elena Díaz-García*[1]*

Conchi O. Ania[2], *José B. Parra*[2]

[1]Department of Physical and Analytical Chemistry, Faculty of Chemistry, University of Oviedo, Av. Julián Clavería, 8, 33006-Oviedo, Spain

[2]Department of Energy and Environment, Instituto Nacional del Carbon, CSIC, PO. 73, 33080-Oviedo, Spain

* To whom correspondence should be addressed: Marta Elena Díaz-García. Tel.: +34 985 10 34 71. Fax: + 34 985 10 31 25. E-mail: medg@uniovi.es

ABSTRACT

Organically modified molecularly imprinted silicas (MIS) for nafcillin recognition were prepared using a simple sol–gel procedure. Molecular recognition of the template was observed by tuning the chemical and structural properties of the MIS. The relative amounts of organically modified alkoxi-sylane precursors were found to be key to develop an imprinting effect and in the textural and morphological characteristics of the MIS. The recognition properties of the imprinted materials were found to be strongly influenced by the hydrolytic stability of the alkoxysilanes and their inductive effects during sol-gel hydrolysis/condensation stages. The concept was to combine properties of organic groups with properties of glass-like materials in order to develop synergetic properties through variations in the composition. Results from batch rebinding experiments and from a thorough study of the N_2 adsorption properties, textural and structural characteristics of the MIS revealed that an imprint effect could be attributed to the presence of the template during the synthesis of MIS.

Keywords: imprinted sol-gels, molecular recognition, binding isotherms, adsorption isotherms

INTRODUCTION

Nowadays, the study of molecularly imprinted materials is a rapidly developing field of research as a means of creating spatial memory of template molecules in highly cross-linked polymeric matrices (Sellergen, 2001; Komiyana et al., 2003; Piletsky and Turner, 2006). In the analytical chemistry arena, molecular imprinting is receiving attention because this methodology provides an approach to synthesize highly substrate- and enantioselective polymers with applications as HPLC stationary phases for chiral resolution, in sensor design, as substitutes for antibodies in immunoassays and for protein separation.

The synthetic imprinting strategies to prepare these materials are inspired by biological structures and their functions. Although most reported molecularly imprinted materials are acrylic-based, the first approaches to synthesize molecularly imprinted materials were based on silica gels prepared by the sol-gel route (MIS). These investigations trace back to the early 1930s with the pioneering work of Polyakov (1931) and to 1949 with the first documented demonstration of nanostructured imprinted silica gels by Dickey (1949). Imprinted sol-gel materials were saved from oblivion and investigations started anew in the 1970s. Different metal oxides (silica and mixed metal oxides), tetralkoxysilanes and organically modified silicas (ormosils) have been imprinted to produce materials with applications as sensing phases, catalysts and adsorbents (Olwill et al., 2004; Guihen and Glennon, 2004; Kunitake and Lee, 2004; Díaz-García and Badía-Laíño, 2005).

The imprinting process consists of three steps: a) selection of the target analyte as template, b) incorporation of the template into a polymer network and c) removal of the template leaving stable, selective cavities that recognize the target analyte. In a self-assembly approach, the template may be directly added a sol-gel solution prior to acid- or basic-catalyzed hydrolysis and condensation. By using organotrialkoxysilane/tetralkoxysilane precursors (or their mixtures) and a fairly polar solvent (e.g. ethanol), imprinted sites may be generated by electrostatic, π-stacking, van der Waals, etc interactions between the template and the sol-gel network. As the solvent evaporates to yield a solid porous material, the imprinted sites are formed by template affinity for the sol-gel matrix. Following a drying step, the gels are extracted with an adequate solvent to remove the template, thus leaving specific receptor sites with a favorable size, shape and chemical environment to selectively rebind the template.

Recognition of a targeted probe using a molecularly imprinted material is crucially dependent on the nature of the host. This is especially true if the selectivity of the recognition process is considered a major goal. Most of the molecularly imprinted materials described in the literature (Bjarnason et al., 1999; Ferrer et al., 2000; Caro et al., 2003; Chapuis et al, 2003; Da Costa Silva et al., 2006) typically contain binding sites that possess a wide range of affinities, which strongly influence their performances. Notwithstanding, the exact nature of the recognition process has been misunderstood in most cases.

Ormosils combine properties of organic groups with those of glass-like materials in order to develop synergetic properties through variations in the composition. The advantages of ormosils over acrylic-based molecularly imprinted polymers (MIPs) include their high thermal stability, the mild temperature conditions for synthesis and that reagents can be readily incorporated in a stable host matrix just by adding them to the sol prior to its gelation. Moreover, the resulting MIS are optically transparent, photo-, electro- and chemically stable, all these properties making these materials ideal for use in optical sensing approaches (Cummins et al, 2005; Díaz-García et al, 2005; Marx and Liron, 2001). In a previous paper, the analytical performance characteristics of different imprinted sol-gels for nafcillin optical sensing (Guardia et al., 2006) were reported. The recognition mechanism based on the interaction between the aromatic moiety of the nafcillin template and the organic moieties in the imprinted sol-gel was proposed taking into account the observed enhanced selectivity of the material. Considering the nafcillin molecular structure, the proposed model encompassed two parallel recognition pathways: i) the interaction of the nafcillin β-lactamic moiety with the sol-gel's silanol groups (through at least two pairs of H-bonds) and ii) the π-stacking interaction between the naphtalenic group of nafcillin and the organic moieties in the imprinted ormosil framework. Nevertheless, a proper understanding of the mechanisms behind the nafcillin recognition process in the imprinted sol-gels is still lacking. To our knowledge none of the studies published in the field of molecular imprinting in hybrid organic-inorganic matrices has provided a conclusive proof of the recognition process. In this paper we describe the molecular imprinting of nafcillin in hybrid organic-inorganic matrices made from of three silicon precursors, namely the tetramethyl orthosilane, the methyl trimethoxysilane and the phenyl trimethoxysilane. Varying the ratio of these precursors, the composition and structure, and thus the properties of the imprinted materials could be tailored. In order to obtain evidence for an imprint effect, the sol-

gels systems were explored by batch rebinding experiments. Also, a thorough study of the N_2 adsorption properties allowed to evaluate the role of the textural and structural characteristics of the MIS on the recognition process.

EXPERIMENTAL SECTION

Preparation of the imprinted sol-gels

The experimental procedure for the synthesis of the imprinted sol-gels has been described elsewhere (Guardia et al., 2006). Briefly, sol-gels were made by mixing an aqueous solution of the template molecule (1140 μL of 1 x 10^{-3} M nafcillin), with 1550 μL of ethanol, and adequate volumes of TMOS (tetramethoxysilane), MTMOS (methyltrimethoxysilane) and PhTMOS (phenyltrimethoxyosilane). Details on the compositions of the gels are compiled in **Table 1.** Gelation of the ormosils was induced by using TBAF (tributylammonium fluoride) as condensation promoter in acid media, during 72 h under ambient conditions, followed by aging at 45 ºC to constant weight for about 2 weeks. Removal of the template was performed by rinsing the materials in 80:20 (v/v) methanol-acetic acid (24 h, 120 cycles) and methanol (8 h, 40 cycles) in a Soxhlet apparatus. An additional batch was prepared using the same procedure, but without the addition of the template (control, non-imprinted silica, NIS).

Textural and structural characterization of imprinted sol-gels

Textural characterization of the imprinted and control sol gels was carried out by measuring the N_2 adsorption isotherms at 77 K in an automatic apparatus (Micromeritics ASAP 2010M) that allowed to control the liquid nitrogen level (within ± 0.2 mm) and the dosing volume deviation (<0.5%). The apparatus was equipped with pneumatically operated control valves (maintained at 25.00±0.05 ºC) and equilibrium pressures were measured with an accuracy of ±0.15% of reading. Before the experiments, the samples were out-gassed under vacuum at 383 K overnight. The isotherms were used to calculate the specific surface area, S_{BET}, total pore volume, V_T, and pore size distributions. The pore size distributions were evaluated using the density functional theory (DFT) (Olivier, 1995). Samples were run in duplicate. Reproducibility of textural analyses was in the 95% confidence level within the range of relative pressures studied. Dry imprinted (and non-imprinted) sol gels were dispersed on a graphite adhesive tab placed on an aluminium stub, coated with a thin layer of gold and

examined with a Ziess DSM 942 scanning electron microscope (SEM). At least, five pictures of each replicate were taken at 500 and 50 x magnification and scanned directly to achieve the SEM image (topographic information). Three independent samples were assayed.

Measurement of adsorption isotherms of nafcillin

Equilibrium isotherm and adsorption kinetic data were obtained in a batch method. Pre-weighed amounts of cleaned MIS and NIS sol-gels (0.01 g) were placed in polyethylene vials containing 2 mL of an aqueous nafcillin solution. The mixture was stirred for 12 h in the dark at room temperature in order to reach equilibrium. Then, the mixture was centrifuged and the left out content of nafcillin in the supernatant solution was determined by heavy atom-induced room temperature phosphorescence, using sodium sulfite 0.015M as oxygen scavenger and KI 1M as heavy atom (Fernandez-González et al., 2003). The amount of bound nafcillin was calculated by subtracting the unbound from total. Initial concentration of antibiotic ranged from 5 $x10^{-5}$ M to 1 $x10^{-3}$ M. Non-specific adsorption was evaluated using the non-imprinted sol-gels that contained the exact same composition of monomer, but in absence of nafcillin in the imprinting stage. All experimental data were the average of three replications of each experiment and the reproducibility of experimental measurements were mostly <7%.

A Perkin-Elmer LS-50B luminescence spectrophotometer which has a xenon discharge excitation source was used for phosphorescence measurement. Further details on the instrumental parameters are described elsewhere (Guardia, L. et al, 2006). The equilibrium data were fitted to several classical adsorption models: Freundlich, Langmuir and bi-Langmuir models (Freundlich, 1906; Langmuir, 1918).

RESULTS AND DISCUSSION

The binding properties of MIS1, MIS2, MIS3 and their corresponding NIS were determined by measuring the nafcillin uptake over a range of concentrations, from 5 x 10^{-5} to 1 x 10^{-3}M, in a batch rebinding approach. Subsequent analysis of the binding isotherm was performed using a log B (B, equilibrium bound nafcillin) versus log F (F, equilibrium free nafcillin) format, a simple test to predict the isotherm model that better fit the experimental data (Umpleby et al, 2004). Isotherms were constructed in triplicate for a constant mass of polymer (0.01g) and results demonstrated that the plots were linear over the entire concentration range for MIS1 and the MIS2 materials, suggesting

a Freundlich model adsorption isotherm (Umpleby et al, 2004). In Figure 1 results for MIS1 and NIS1 are depicted. On the contrary, for MIS3, the isotherms were curved over the whole range of concentrations studied (see Figure 2), which suggested a Langmuir model adsorption process (Umpleby et al, 2004). Fitting of the data to theoretical models (Freundlich, Langmuir, bi-Langmuir) that accounted for the experimental facts was then performed. Isotherm constants were determined by linear regression and the results of the calculated constants and the correlation coefficients are compiled in Table 2, for both the MIS and NIS series. The high linear regression coefficients (above 0.98) indicated that the Freundlich isotherm provided a reasonable description of the experimental data for interaction of nafcillin with the MIS1 and MIS2, while for the interaction of nafcillin with MIS3, the correlation coefficient was below 0.7. However, when the bi-Langmuir model was considered a linear regression coefficient higher than 0.99 was found for the MIS3 (see data in Table 2).

The heterogeneity parameter, *m*, is a measure of the ratio of high-to-low affinity sites, that is, it is a measure of the percentage of high-affinity sites and varies from zero to one (values approaching zero indicate increasing heterogeneity whereas values close to unity show homogeneous surfaces). In the systems under study, the MIS1 (and its corresponding control) showed higher values of *m* than the MIS2 sol-gel, for the binding of nafcillin, which indicated a lower percentage of high-affinity binding sites. On the other hand, the lower values of *m* for the binding of nafcillin to MIS2 (and its corresponding control) indicated a more heterogeneous material with a higher percentage of high-affinity binding sites. In contrast, the binding capacities of the MIS2 and its control were lower than those of the MIS1 and its corresponding control. In order to compare the heterogeneity indexes of imprinted and non-imprinted sol-gels, a t-test was performed, adopting the null hypothesis that there was no significative difference in the mean *m* values (Miller and Miller, 2000) and a Fisher test was used as reference. For 22 degrees of freedom, the experimental value of $|t|$ ($P = 0.05$) was 4.193. Since the critical value of $|t|$ for $P = 0.05$ was 2.074 (Bauer, 1974), the difference between the two *m* values was significant at the 5% level and the null hypothesis was rejected. This indicated that the MIS1 was more heterogeneous than its NIS1 counterpart, while the NIS2 resulted to be more heterogeneous than the corresponding MIS2, as confirmed by the adsorption data (binding capacity for NIS2 resulted to be three times higher than that of MIS2).

In Figure 3 the bi-Langmuir binding isotherms for the MIS3 sol-gel and the corresponding control sol-gel are shown. Although a heterogeneity index can not be obtained for this material by using a Langmuir-type model, the fact that experimental data fitted to this model seemed to indicate a more homogeneous distribution of binding site classes in this imprinted sol-gel when compared with the imprinted MIS1 and MIS2 materials. The binding parameters were obtained using the linearized form of bi-Langmuir equation (inset in Figure 3). At least, two different kinds of adsorption sites were present in MIS3, which behaved independently, and on each of which a different Langmuir model applied. Assuming that no template-template interactions were working, the first term of the bi-Langmuir isotherm may explain the high energy binding sites against nafcillin and the second term the non-specific interactions between MIS3 and nafcillin. Support for this was the high affinity constant of the imprinted material (i.e., 530 *vs* 11) obtained in the first part of the isotherm, as opposed to the much lower values obtained when the model was applied to the second part of the isotherm (57 *vs* 1.6) (see Table 2). The MIS3 and its control showed binding capacities ranging between those of MIS1 and MIS2.

In order to assess the template recognition performance of the sol-gels the *imprinting factors* were calculated as the ratio K_{MIS}/K_{NIS}, where K_{MIS} and K_{NIS} are the value of affinity constant for the MIS and NIS sol-gels, respectively. The value of affinity constant for MIS1 and MIS3 sol-gels were larger than those for non-imprinted ones (i.e., larger imprinted factors), demonstrating the higher affinity of these materials for nafcillin than their corresponding non-imprinted ones (see Table 2), particularly in the case of the MIS3. The imprinting factor was even more conspicuous for the MIS3 sol-gel, for which it was about one order of magnitude. The case of the MIS2 resulted to be quite different, having the non-imprinted control sol-gel a higher affinity constant for the nafcillin than the imprinted material. The main difference in the composition among the materials under study was the molar ratio of the organically modified alkoxysilanes. This ratio, defined as [MTMOS+PhTMOS]/[TMOS], is a measure of the degree of organic functionalization of the sol-gel materials. As can be seen in Table 1, the molar ratio was about 50 and 10 times higher for the MIS3 sol-gel than for the MIS1 and the MIS2, respectively, indicating a different hydrophobic/hydrophilic character of MIS3. These results indicated that (partial) replacement of TMOS by MTMOS in the precursor mixture favoured a clear imprinting effect. Also, it is worth noting that previous results (Guardia et al., 2006) demonstrated that the selectivity of the binding sites of the

imprinted sol-gels against nafcillin (in comparison with other β-lactamic antibiotics) was related with a higher degree of organic functionalization of the inorganic network. A plausible explanation of these facts may be related with the kinetics of the nucleation process at the early stages of the sol-gel process. Taking into account that organically substituted alkoxysilanes $RSi(OR)_4$ are more reactive than the corresponding $Si(OR)_4$ under acidic conditions (Schubert and Hüsing, 2000), the rate of the hydrolysis and condensation reactions may be different for MIS3 with a molar ratio [MTMOS + PhTMOS]/[TMOS] much higher than that of MIS2 or MIS1.

The electronic effects of the organic group play also a key role as they stabilize or destabilize the transition states during hydrolysis and condensation. Under acidic condictions, the hydrolysis of alkoxysilanes is reported to be initiated by the fast protonation of a leaving alkoxy group. Subsequent nucleophilic attack of water molecule leads to a five-coordinate transition state (Wright and Sommerdijk, 2001). The substitution of an alkoxy group with an alkyl group increases the hydrolysis rate by stabilizing the development of positive change by providing electrons (polar effect) while gelation may be retarded due to the lower steric hindrance of an alkyl group compared to an alkoxy group (steric effect). Thus, the electron density at the silicon atom decreases in the following order: ≡Si-R > ≡Si-OR > ≡Si-OH > ≡Si-O-Si (Schubert and Hüsing, 2000). Thus, according to the polar effect the reaction rates for hydrolysis and condensation should increase in the order MIS3 > MIS2 > MIS1. Due to the different mechanisms, formation of a three-dimensional inorganic network around the template seemed to be favoured in the case in which the transition state was stabilized (MIS3 > MIS2 > MIS1). Finally, it is known that introduction of non-hydrolysable substituents (methyl- phenyl-) lowers the connectivity of the network by leaving “dead ends” (Wright and Sommerdijk, 2001). These “dead ends” (organic groups) were retained during hydrolysis and their higher proportion in MIS3 (higher [MTMOS+PhTMOS]/[TMOS] ratio) compared to MIS1 and MIS2, served to create an organic-inorganic building block around nafcillin in MIS3 thus resulting in a higher imprinting factor for this material (see Table 2).

Characterization of the sol gels

In our knowledge, the nature of non-specific interactions in imprinted sol-gels has not been linked to the porosity and textural morphology of the aero-gels, thus obviating an issue of prime importance in most adsorption processes. As the presence of such non-

specific interactions may reduce and/or obscure an imprint effect, thus limiting the practical utility of the imprinted sol-gels (Guardia et al., 2006), we have investigated the characteristics of these materials from a structural point of view. For this purpose, the porosity of the samples was evaluated by N_2 adsorption-desorption measurements at cryogenic temperature. Figure 4 depicts the N_2 adsorption-desorption isotherms for the three imprinted sol-gels. Experimental errors for replicate measurements were lower than 0.5% within the whole range of relative pressures. It was interesting to observe that similar isotherms were obtained for the corresponding control sol-gels, which indicated that the presence of the template (i.e., nafcillin) during the synthesis of the sol-gels did not exert any influence on the porous network of the resulting materials. In turn, the porosity seemed to depend strongly on the [MTMOS+PhTMOS]/[TMOS] molar ratio and/or the nature of the functional precursors used during the sol-gel preparation. On the other hand, the shape of the isotherms also changed with the [MTMOS+PhTMOS]/[TMOS] molar ratio. The MIS3 sol-gel, the material with a higher degree of organic functionalization, presented lack of porosity (at least accessible to nitrogen molecules at 77 K), while the most hydrophilic MIS1 displayed a type I isotherm according to the BDDT classification (Brunauer et al., 1940), indicating a mainly microporous nature of this polymer. The MIS2 sol-gel, with an intermediate [MTMOS+PhTMOS]/[TMOS] molar ratio, presented a well-developed microporosity. The isotherm shape was a combination of type I/IV (characteristic of materials with a well-developed mesoporosity), showing an increase in the volume of adsorbed N_2 at relative pressures above 0.6. The prominent hysteresis loop at relative pressures between 0.5-0.9 was indicative of pores containing constrictions (narrow necks and wide bodies or ink bottle pores), commonly found in silica gels.

Detailed characteristics of the pore structure of the series of sol-gels are presented in Table 3. It is interesting to notice that the BET surface area did not change significantly between the imprinted and the corresponding NIS materials. This fact suggested that the porous features of the materials were not dependent on the presence of the template molecule but on the chemical composition of the silica materials. BET surface area decreased with increasing the [MTMOS+PhTMOS]/[TMOS] molar ratio of the materials, showing the MIS3 sample the lowest value (i.e., 7 m^2g^{-1}) compared to MIS1 and MIS2. This material also presented the lowest pore volumes (including micro and mesopores).

The pore size distributions of the materials, obtained by applying the DFT model to the N_2 adsorption data are compiled in Table 3. Both, the micropore and mesopore volumes were much higher in MIS1 and MIS2 samples than in MIS3. The control samples presented identical porous features than their corresponding imprinted counterparts. Similar trends could be observed for the surface area of these materials. Comparatively, MIS2 exhibited the largest mesopore volume, more than 2 times higher than the micropore volume. This fact was in good agreement with the shape of its nitrogen isotherm, as aforementioned. Hence, it seemed that a relationship existed between the porosity of the sol-gel materials and their hydrophobic/hydrophilic nature. Particularly, poor porosity development was observed in those samples with the higher [MTMOS + PhTMOS] / [TMOS] molar ratio (e.g. MIS1 and NIS1). The low porosity development in materials with a higher degree of organic functionalization may be attributed to a reduction in the connectivity of the network ("dead ends") brought about by the incorporation of methyl/phenyl groups in the alkoxysilane used as precursors.

Additional differences between MIS and NIS series were seen in the morphology of the particles by means of SEM, regardless the presence or absence of nafcillin in the synthesis of the materials. Micrographs confirmed that whereas MIS1 and MIS2 presented a dense (solid) structure (Figure 5), the sol-gel with the higher [MTMOS + PhTMOS] / [TMOS] molar ratio (MIS3) displayed two well-defined morphologies. The presence of globular structures in form of spherical particles with an average size of 500 μm and solid particles characterized by the presence of micro voids are clearly observed in Figure 6 for MIS3. Such morphological features were not observed in the materials with lower [MTMOS+PhTMOS]/[TMOS] molar ratios. It seemed that the presence of large amounts of organically-modified precursors served to increase the spacing between growing colloidal particles and hence to reduce coagulation rates. Moreover, cross linking of the polymer became more restricted with the incorporation of pendant ligands and therefore, a less porous 3 D structure was favored corroborating thus the results from gas adsorption data. The presence of these two different types of particles for MIS3 did not affect the reproducibility of the binding process as we could assess during the continuous use of this material as sensing phase for nafcillin (L.Guardia et al., 2007).

From the performance of the sol-gels against nafcillin, it was clear that the architecture of the materials played a key role in the recognition process. It was important to maintain a cross-linked network in the sol-gels but preventing an over-

expansion of the matrix during the condensation step. As aforementioned, the development of porosity constituted an additional source for non-specific interactions, thus resulting that retention of nafcillin on the sol-gels that exhibited a porous network was not based on a molecular recognition of the template but on typical adsorptive forces. Based on these results, the different behavior of the sol-gels against nafcillin may be explained in terms of porosity development. The large binding capacities of the NIS1 and NIS2 were due to non-specific adsorption arising from their well-developed porous network. Both materials presented the micropores acting as active sites for nafcillin adsorption. In contrast, the lack of porosity in MIS3 prevented the non-specific adsorption being thus the imprinting factor of this material higher than that of NIS3.

CONCLUSIONS

Imprinted microporous silica showed unforeseen nafcillin recognition ability depending on the nature and the relative proportion of the alkoxy precursors used in their preparation when the template molecule was present. Batch rebinding isotherm experiments demonstrated that not only the imprinting factor but also the heterogeneity of the binding sites increased as the organic functionalization of the resulting material increased. When compared with control sol-gels prepared in the absence of the template, the binding affinity and molecular recognition of the more functionalized sol-gels were related to imprint effects. On the other hand, the binding of nafcillin to the sol-gels with a low degree of organic functionalization was attributed to non-specific interactions resulting from changes in surface polarity of the final materials that, in turn, obscured any imprinting effect.

By exploring the porous network nature of the materials, new light was shed on the imprinting process. A correlation between the hydrophobic/hydrophilic character of the silica sol-gels and their microstructure was found. While no porosity and an almost negligible BET surface area were observed for the more organically functionalized material prepared (MIS3), relatively high surface areas and micro/mesoporosity were observed for the low-functionalized ones (MIS1 and MIS2). The textural properties of the gels measured by SEM were also found to depend on the degree of organic functionalization of the material, leading to vastly different morphologies. In fact, SEM indicated maximum heterogeneity in the MIS3 material, with spherical morphology in the nano-range and voids in the micro-range. As the control materials showed similar

porosity and textural properties as their imprinted counterparts, the enhanced affinity of the MIS3 over the NIS3 could be attributed to the presence of the template during the synthesis of the MIS3 and not to a change in the micro/nanostructure of the material itself. We believe that favourable interactions between the template and the alkoxysilanes during the preparation of imprinted silicas, tuned by adequate selection of precursors, were responsible for creating an imprint effect in the hydrophobic MIS3. It should be noticed that the outstanding recognition characteristics of the MIS3 (i.e., the imprint effect, selective recognition and stability) were kept even under different experimental conditions, which allowed its use for the flow injections room temperature phosphorimetric sensing of nafcillin in real, complex matrixes (Guardia et al., 2007).

ACKNOWLEDGMENTS

Authors gratefully acknowledge financial support to the Spanish Science and Education Ministry (Projects #BQU2003-00853 and CTQ2006-14644-C02-01). L Guardia thanks FICYT (Foundation for Scientific and Technological Research, Principado de Asturias) for support (Pre-doctoral Grant). COA thanks CSIC (I3P contract) co-financed by the European Social Fund, for a postdoctoral contract.

REFERENCES

Bauer, E.L., 1974. Manual de Estadística para Químicos; Ed.Alhambra, Spain.

Bjarnason, B., Chimuka, J. Ramstrom, O., 1999, Anal.Chem., 71, 2152-21

Brunauer, S., Deming, L.S., Deming, W.E., Teller, E., 1940. J. Am. Chem. Soc., 62, 1723-32.

Caro, E., Marce, R.M., Cormack, P.A.G., Sherrington, D.C., Borrull, F., 2003. J. Chromatogr. A 995, 233-238.

Chapuis, F., Pichon, V., Lanza, F., Sellergren, V., Hennion, M.C., 2003. J. Chromatogr. A 999, 23-33.

Cummins, W., Duggan, P., McLoughlin, P., 2005. Anal. Chim. Acta 542, 52-60.

Da Costa Silva, R.G., Augusto, F., 2006. J. Chromatogr. A, 1114, 216-233.

Díaz-García, M.E., Badía-Laíño, R., 2005. Microchim. Acta, 149, 19-36.

Dickey, F.H., 1949. The preparation of specific adsorbents. Proc. Natl. Acad. Si. USA, 35, 227-229

Fernandez-González, A., Badía, R., Dıaz-Garcıa, M.E., 2003. Anal. Chim. Acta 498 (1–2), 69-77.

Ferrer, I., Lanza, F., Tolokan, A., Horvath, V., Sellergren, B., Horvai, G., Barcelo, D., 2000. *Anal. Chem*. 72, 3934-3941.

Freundlich, H.M.F., 1906, *Zeitschrift für Physikalische Chemie* 57, 385–470.

Guardia, L., Badıa, R., Dıaz-Garcıa, M.E., 2006. *Biosensors Bioelectronics* 21, 1822–1829.

Guardia, L., Badía, R., Díaz-García, M.E., 2007. J. Agric. Food Chem, 55(3), 566-570

Guihen, E., Glennon, J.D., 2004. J. Chrom. A, 1044, 67-81.

Komiyama, M., Takeuchi, T., Makawa, T., Asanuma, H., 2003. Molecular imprinting. From fundamentals to applications. Wiley-VCH, Winheim, Federal Republic of Germany.

Kunitake, T., Lee, S.-W., 2004, Anal.Chim.Acta, 504, 1-6

Langmuir, I., 1918. J. Am. Chem. Soc, 40, 1361-1368.

Marx, S., Liron, S., 2001. Chem. Mater. 13, 3624-3630.

Miller, J.C., Miller, J.N., 2000. *Statistics and Chemometrics for Analytical Chemistry* (4th Ed). Prentice Hall, Edinburgh, U.K.

Olivier, J.P., 1995. J. Porous Mater. 2, 9-17.

Olwill, A., Hughes, H., O'Riodain, M., McLoughlin, P., 2004. Biosensor Bioelectr., 20, 1045-1050.

Piletsky, S., Turners, S.A. (eds.) 2006. *Molecular imprinting of polymers*. Landes Bioscience. Georgetown, Texas, USA.

Polyakow, M.V., 1931. Zhur. Fiz. Khim, 2, 799-805

Schubert, U., Hüsing, N., 2000. *Synthesis of Inorganic Materials*. Wiley-VCH. Weinheim, FRG.

Sellergren, B., (Ed.), 2001. *Molecularly imprinted polymers. Man-made mimics of antibodies and their applications in analytical chemistry*. Elsevier, Amsterdam.

Umpleby II, R.J., Baxter, S.C., Rampey, A.M., Rushton, G.T., Chen, Y., Shimizu, K.D., 2004. J. Chromatogr. B, 804, 141-149.

Wright, J.D.; Sommerdijk, N.A.J.M;, 2001. *Sol-gel Materials. Chemistry and Applications*. CRC Press; Boca Ratón. Florida.

Figure 1. Experimental binding isotherms for MIS1 (a) and NIS1 (b)

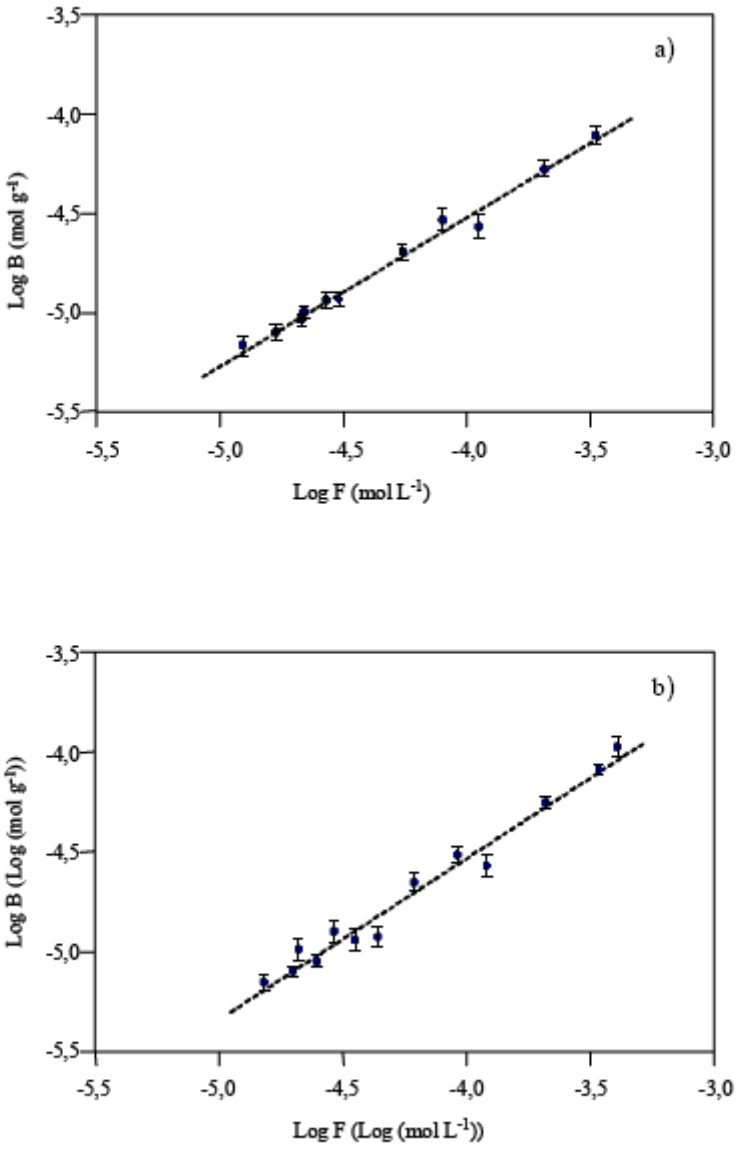

Figure 2. Experimental binding isotherms for MIS3 (a) and NIS3 (b)

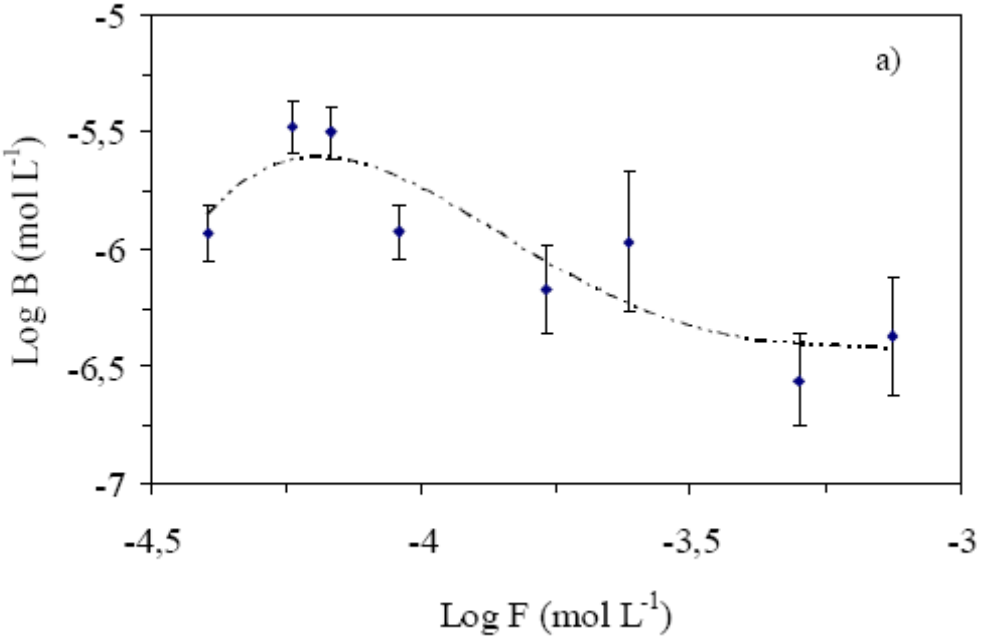

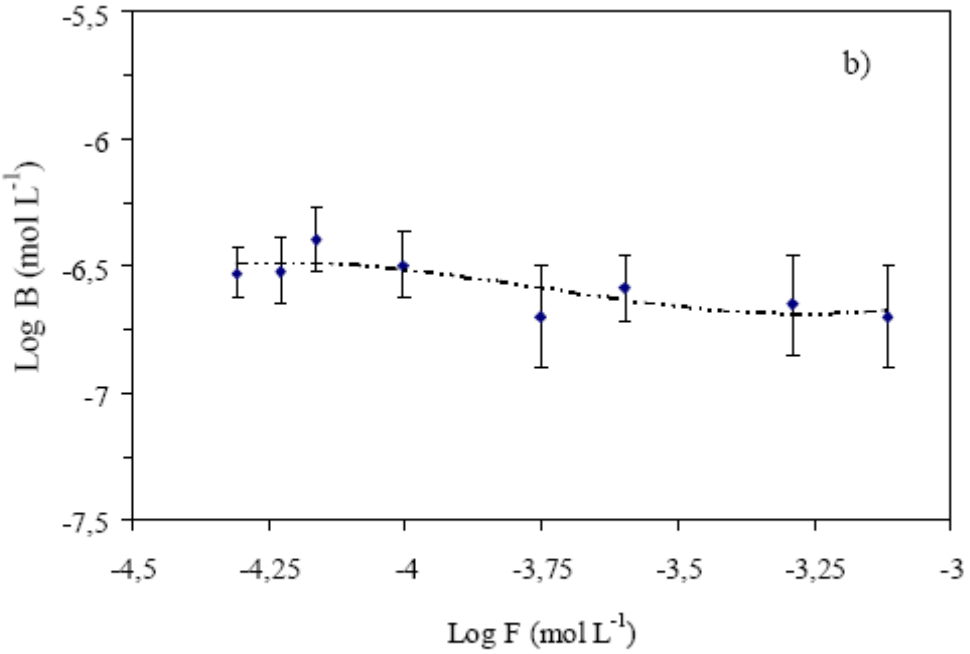

Figure 3. Bi-Langmuir binding isotherm for MIS3

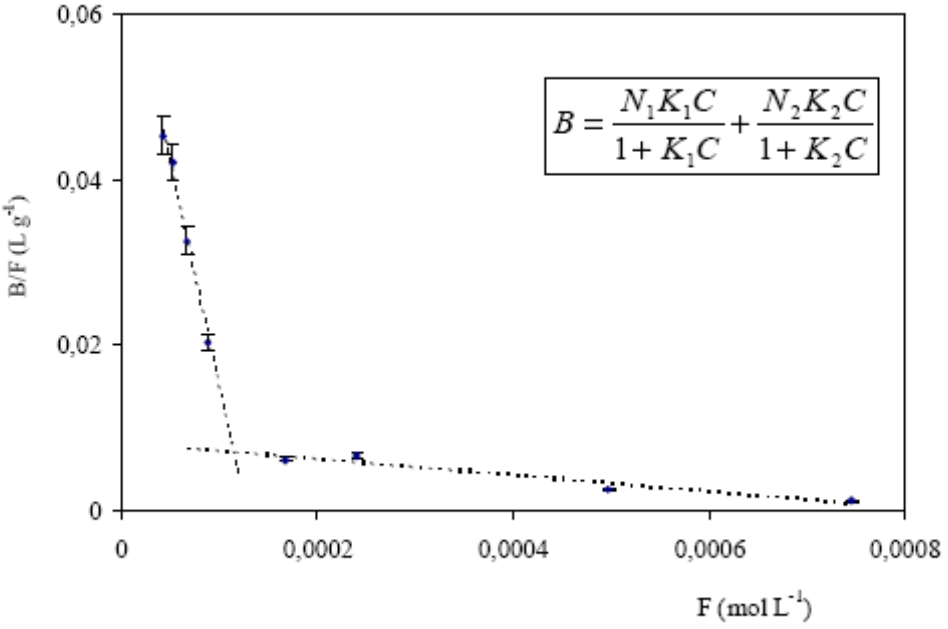

Figure 4. N_2 adsorption isotherms at -196ºC of the imprinted and non-imprinted sol-gels

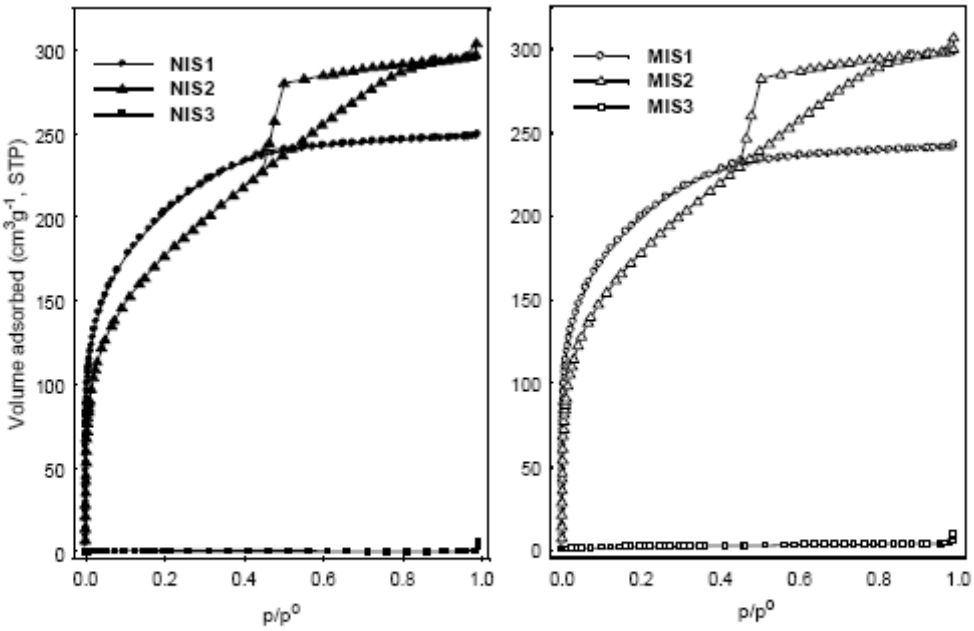

Figure 5. SEM micrographs at 500 and 50 μm magnification, showing a) MIS1 particles, b) material MIS2 particles

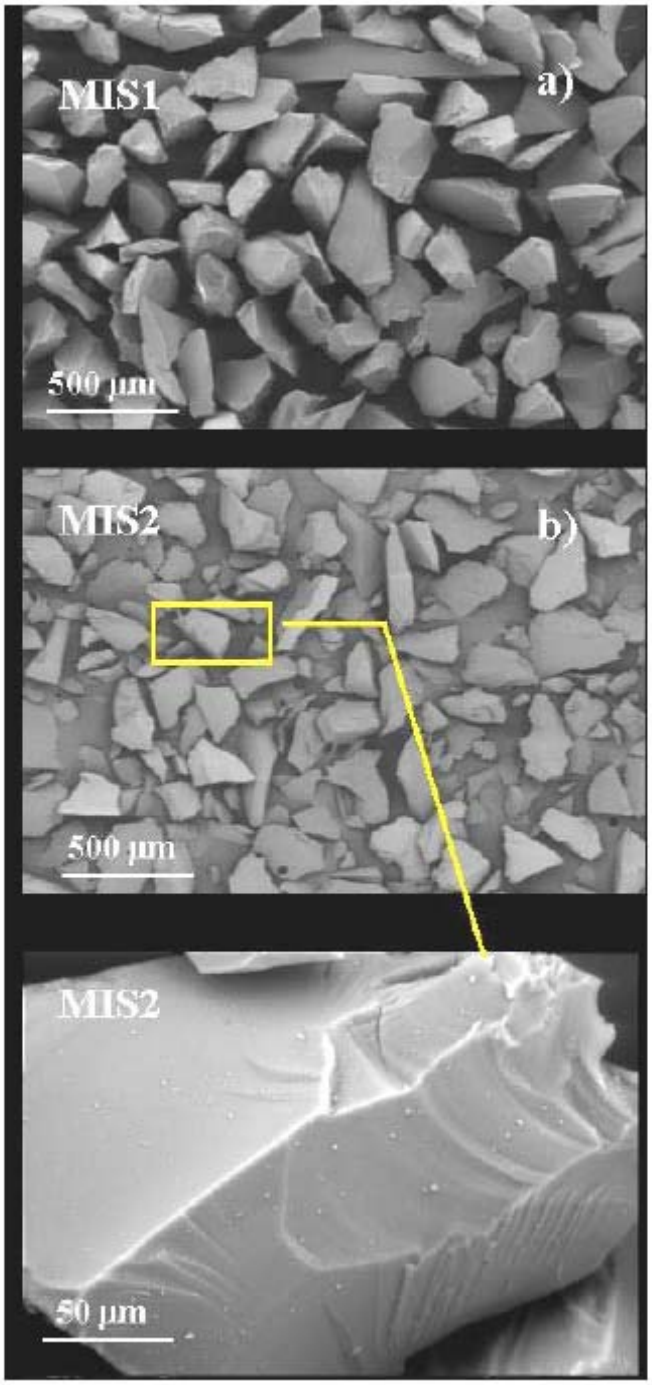

Figure 6. SEM micrographs at 500 and 50 μm magnification, showing MIS3 spherical and porous particles.

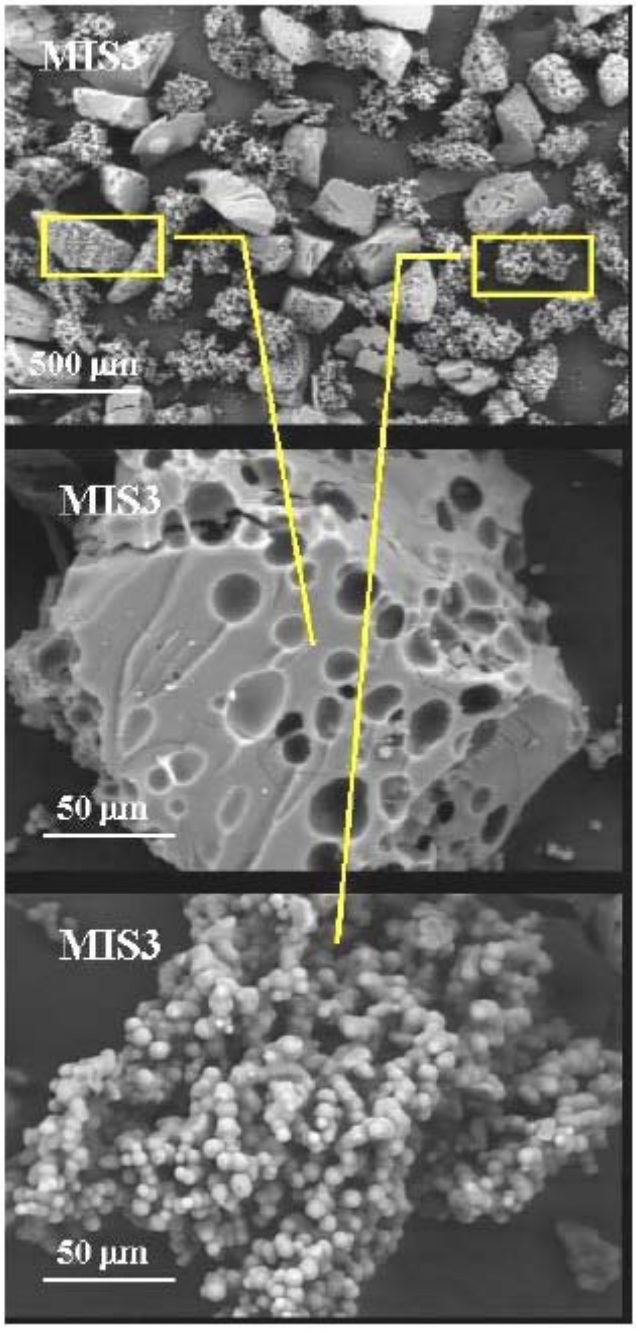

Table 1 Composition of sol-gel materials

Sol-Gel	*MTMOS (µL)*	*TMOS (µL)*	*PhTMOS (µL)*	$\frac{MTMOS + PhTMOS}{TMOS}$ *Molar ratio*
MIS1	120	1230	150	0.22
MIS2	675	675	150	1.22
MIS3	1230	120	150	11.5

Table 2. Isotherm fitting parameters of nafcillin imprinted (MIS) and non-imprinted (NIS) sol-gels

Isotherm model	*Sol-gel material*	*Affinity constant, K (M^{-1})*	*Binding site density, N x 10^4 (mol g^{-1})*	*Heterogeneity parameter, m*	*Binding capacity K x N ($g L^{-1}$)*	*Regression coefficient, R^2*	*Imprinting factor K_{MIS}/K_{NIS}*
Freundlich	MIS1	(5.4 ± 2.0) x 10^4	0.033 ± 0.001	0.73 ± 0.03	1782 ± 660	0.980	1.1 ± 0.6
	NIS1	(5.1 ± 2.3) x 10^4	0.028 ± 0.001	0.80 ± 0.05	1428 ± 644	0.960	
Freundlich	MIS2	(6.2 ± 1.8) x 10^3	0.001 ± 0.002	0.62 ± 0.03	5.6 ± 1.6	0.997	0.3 ± 0.1
	NIS2	(9.1 ± 3.1) x 10^3	0.002 ± 0.001	0.49 ± 0.02	17.3 ± 5.9	0.996	
Bi-Langmuir	MIS3	K_1 = 530 ± 83 K_2 = 11 ± 4	N_1 = 1.3 ± 0.3 N_2 = 7.4 ± 0.4	-	689±193 81.4 ± 30	0.997 0.940	9.3 ± 3.2
	NIS3	K_1 = 57 ± 17 K_2 = 1.6 ± 0.2	N_1 = 1.6 ± 0.7 N_2 = 8.6 ± 0.6	-	91.2± 48 13.8± 1.9	0.960 0.970	6.9 ± 2.6

Table 3. Textural parameters of the imprinted (MIS) and non-imprinted (NIS) sol-gels, obtained from the N_2 adsorption data at -196 ºC.

Sol-gel material	S_{BET} (m^2g^{-1})	V_{TOTAL}* (cm^3g^{-1})	$V_{micropores}$** (cm^3g^{-1})	$V_{mesopores}$** (cm^3g^{-1})
MIS1	734	0.373	0.202	0.121
NIS1	745	0.365	0.203	0.129
MIS2	659	0.481	0.144	0.266
NIS2	655	0.477	0.143	0.264
MIS3	7	0.017	0.001	0.005
NIS3	7	0.015	0.001	0.005

* total pore volume evaluated at p/po > 0.99
** evaluated by DFT method